Journal of Electrical Engineering, Vol. 74, No. 3, 2023, pp. 228-239

sciendo

PAPER

New design and optimization of an in-wheel permanent magnet motor with tangentially magnetized magnets and unequal stator teeth

Lassaad Zaaraoui, Ali Mansouri

Permanent magnet synchronous machines (PMSM) are competitive motors for in-wheel traction systems of electric vehicles. A new tangentially magnetized permanent magnets machine with outer rotor and unequal stator teeth for in-wheel motor application is proposed in this paper. The analytical calculations of the proposed topology are presented by determining the magnetic flux densities and the iron losses in all parts of the machine. The machine design is optimized using three state-of-the-art multiobjective algorithms which are AbYSS, MOCell and NMOPSO algorithms. Moreover, the optimization procedure is carried out according to three objectives: the maximization of the machine efficiency and the minimization of the mass and ripple torque. The optimization results showed that all the algorithms can find a set of optimal solutions and that the NMPSO algorithm outperforms the other two techniques. The finite element method (FEM) is used to investigate the optimization results. It is observed some magnetic saturation in the rotor yoke and the magnet's extremes. The value of the induction in these machine regions is about 1.9 T. The comparison between the FEM and optimization results proved the rationality of the proposed optimization procedure.

Keywords: In-wheel motor, tangentially magnetized permanent magnets, unequal stator teeth, multiobjective optimization, finite element method

1. Intorduction

The planet's natural resources are currently overexploited and the steady increase in toxic emissions could spell ecological catastrophe if no global action is taken. The transport sector is one of the main sectors responsible for global CO_2 emissions since most vehicles use motors powered by petroleum derivatives.

Today, electric vehicles have been recognized globally as the most ecological road transport. For the propulsion systems, the electric motors are used instead of internal combustion engines to minimize the pollution, save the fossil fuels consumption and to improve the vehicles performances. Moreover, it is widely recognized that the most attractive motorization technology for the propulsion of electric vehicles is that of PMSM [1]. The greatest advantages of PMSM are [1,2]: high power density, low volume, light weight, high dynamic performance, and very low maintenance required.

Depending on the application, we can distinguish several PMSM topologies. Indeed, these topologies can be distinguished according to the magnetic flux direction, the rotor position, the location of the permanent magnets, the stator structure, and the type of the stator windings. In this work, the intended application is an in-wheel motor for the traction of electric vehicles. The main advantages of the in-wheel motor are [2,3]: the power, braking and transmission are integrated into the wheel hub which makes the structure more compact, the volume of the vehicle interior is reduced, the traditional mechanical transmission are discarded which reduces the mechanical loss, the performance of the whole vehicle is improved, driving safety and stability.

Over the last few years, various works focus on the optimal design and the evaluation of permanent magnet synchronous motors for drive applications [4,5]. Indeed, in [6], a multiobjective optimization design of an outer rotor permanent magnet hub motor for an electric vehicle is carried out. A set of constraints related to the driving conditions are considered during the optimization. Moreover, the FEM and temperature network model are applied to verify the accuracy of the optimization results. It has been shown that the proposed multiobjective optimization can improve the motor efficiency, reduce the torque ripple, and ensure the temperature rise of the motor in a reasonable range. In addition, the FEM and temperature network model showed that the accuracy of the optimization results is reliable. Finally, a prototype of the proposed motor is manufactured and analyzed using test benches. The experimental results showed that the test results of prototype agree with the simulation design results.

In [7], a dual rotor permanent magnet in-wheel motor with toroidal winding is designed and analyzed. Firstly, the topology and some significant design considerations of the studied machine are investigated. Indeed, the sizing equation and the reduction of torque pulsation and cogging torque are analyzed. Finally, FEM is used to predict electromagnetic performance of the studied machine.

Two in-wheel permanent magnet synchronous motors for electric vehicles application are analyzed and investigated in [8]. The topologies of these motors are: surface-mounted permanent magnet motor (SPM) and interior permanent magnet motor (IPM). Firstly, the main design parameters of both motors are presented. Then, FEM is used to analyze motor loss and electromagnetic performance of both motors. The FEM results confirm that both motors are qualified for the electromagnetic performance requirements. Moreover, through thermal analysis, magnet segmentation is adopted to minimize eddy current loss. Indeed, the thermal performances of both

University of Gafsa, Faculty of Sciences of Gafsa, Laboratory of Technology, Energy, and Innovative Materials, Tunisia
lassaad.zaaraoui@gmail.com, ali.mansouri@isetgf.rnu.tn

https://doi.org/10.2478/jee-2023-0029, Print (till 2015) ISSN 1335-3632, On-line ISSN 1339-309X

motors with segmented and non-segmented magnets are analyzed. This comparison showed that the IPM has the better thermal performance compared to SPM.

In [9], a novel variable-flux outer rotor permanent magnet in-wheel motor is developed. The design of this machine is proposed with a hybrid magnetic structure using Nd-Fe-B and Al-Ni-Co permanent magnet to realize both high torque density and flux adjustment. Firstly, the basic structural features of the motor and the principle of flux adjustment are presented. Then, the design of the magnet dimensions is derived based on magnetic circuit analysis. After that, the hysteresis model of Al-Ni-Co magnet is used in combination with the time-step FEM to analyze the motor performance, and the magnetizations are investigated. Finally, finite element simulations are performed to prove the rationality of the proposed motor design.

A new dual-stator and dual-field-excitation permanent magnet in-wheel motor is presented in [10]. The studied machine is based on both the conventional in-wheel motor and the axial flux permanent magnet machine. Firstly, the structure of the studied machine is described. Then, the design of the machine is presented based on the structural dimensions of an in-wheel motor. Finally, FEM is used to analyze the back electromotive force, electromagnetic torque, and mechanical characteristics of the studied motor. The results showed that the studied machine has higher power at high speed, higher torque at low speed, and a lower torque ripple.

In the literature, stochastic optimization algorithms are widely used in PMSM optimization. Indeed, in [11], an optimized design of a double rotor axial flux PMSM for electrical vehicles is achieved by using genetic algorithm. The sizing equations and the magnetic circuit model of the studied motor are determined. With the help of MATLAB program, an optimization procedure is performed with the genetic algorithm. As a result, the optimal geometry and the motor performance are carried out.

In [12], the non-dominated sorting genetic algorithm II (NSGA-II) coupled with a hybrid analytical/finite element model is used to optimize the design of a spoke-type interior PMSM for electric vehicle. The aim is to optimize the geometry of the machine to obtain the highest torque and efficiency values without exceeding the material's withstanding temperature or saturating the magnetic core. The optimization procedure is carried out under geometrical, thermal and magnetic constraints. The optimization results showed that it is possible to obtain a motor design with 20 Nm of torque and 98.6% of efficiency. The final motor with the optimized design was built and tested. It was registered a torque of 18.2 Nm and an efficiency 90% for the developed prototype.

In [13], a multiobjective optimization design of a permanent magnet in-wheel motor is carried out by using the adaptive weighted particle swarm optimization algorithm (AWPSO). The optimization target is to reduce electromagnetic vibration and cogging torque while maintaining a high output torque. The optimized design is compared and verified by FEM. The investigation showed that the vibration and cogging torque can be reduced simultaneously with improvement of output torque by the adjustment of the pole-slot structure parameters which are: PM thickness, pole-arc coefficient, slot opening width and stator slot width.

In [14], an optimization of a surface PMSM is performed by particle swarm optimization (PSO) algorithm. The aim is to minimize the copper losses and solve the heating problem. To achieve this goal, the parameters of the windings in the stator are optimized. The PSO results showed that the heating problem is solved and the copper losses of the motor are reduced from 0.719 W to 0.4684 W. Moreover, an RMxprt analysis of the studied motor is carried out. Analyzes showed that the optimized design can reduce the torque ripple in the motor. Finally, the simulation results of the optimized design are verified by the experimental results.

This paper is devoted to the geometry optimization and the performance evaluation of a new permanent magnet in-wheel motor. Indeed, we are interested in a buried permanent magnet motor with an external rotor and unequal stator teeth. Firstly, the machine topology and the main analytical calculations of the studied machine are described. Secondly, the optimization algorithms applied in this work are presented. Then, the optimization results of the motor are presented, and discussed. Finally, we use FEM to investigate the performance of the motor.

2. Design of the machine

2.1 Machine topology

In this study, the machine topology is a 3-phase, 18 slots, and 16 tangentially magnetized permanent magnets with an outer rotor and unequal stator teeth lapped with single-layer concentrated windings. This motor is designed to be mounted inside the wheel for the traction of electric vehicles.

The outer rotor is widely used in the design of in-wheel motor since it corresponds to a large radial diameter that can accommodate a large number of poles, which increases the torque density. Moreover, this configuration gives good mechanical strength to the machine [15]. The rotor is made of different pieces of iron and permanent magnets which are fixed together on a non-ferromagnetic shaft to decrease the leakage flux.

The permanent magnets are buried inside the rotor lamination and tangentially magnetized (Fig.1). This configuration makes it possible to offer good protection of the magnets against the risk of detachment, thus improving the mechanical integrity to resist centrifugal forces. Moreover, this configuration enhances the machine output torque [16].

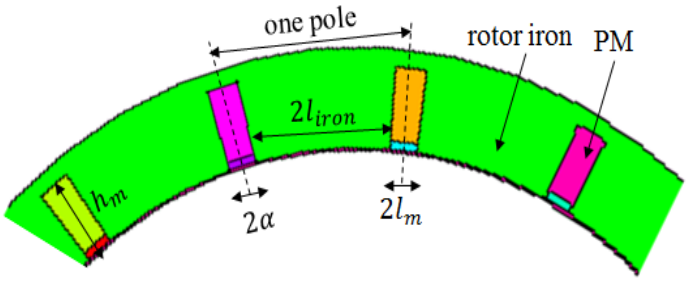

Fig. 1. Tangentially magnetized PM rotor

Furthermore, we have specifically focused our selection on the machine with unequal stator teeth without tooth tips since it has the best performance compared to conventional stator structures like modular stator and equal stator teeth. In fact, this structure can increase the electromagnetic torque, decrease the torque ripple, the copper losses, and the motor mass, and improve the fault tolerance capability [17]. In [18], the cogging torque reduction of a permanent magnet synchronous motor was carried out by means of genetic algorithm.
In the literature, double layer and single layer concentrated windings can be applied. In our work, single-layer concentrated windings are selected as an arrangement of the stator winding. For a machine with unequal stator teeth, this configuration is more suitable than distributed and double layer windings. Indeed, the concentrated winding arrangement increases the performance of the machine, minimizes the copper and iron losses, and reduces the mass of the machine [2]. The advantage of using a single-layer winding is that the machine can have a higher self-inductance which makes it possible to limit the short-circuit currents. Moreover, this configuration increases the average torque and reduces the torque ripple. The single-layer concentrated windings should be wound on the wider teeth to achieve a higher winding factor.

The machine structure is shown in Fig. 2 and the main geometrical parameters of the machine are presented in Table 1.

Table 1. Geometrical parameters of the machine

Parameters	Symbols	Bounds
Airgap length (mm)	δ	[1; 1.5]
Permanent magnet length (mm)	h_m	[20; 40]
Half pole angle (°)	α	[2; 4]
Widest stator tooth width (mm)	b_{ts1}	[26; 30]
Narrowest stator tooth width (mm)	b_{ts2}	[19; 21]
Stator slot height (mm)	h_s	[30; 40]
Axial machine length (mm)	l	[60; 85]
Stator inner diameter (mm)	D_{sint}	[115; 122]

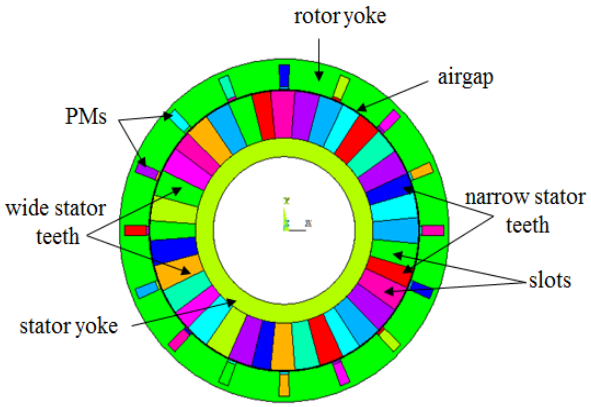

Fig. 2. Machine structure

2.2 Analytical calculations

In this section we present the analytical calculations of the magnetic flux densities and the iron losses in all parts of the motor. Indeed, the maximum value of the airgap flux density created by the permanent magnets (B_m), can be expressed by the following equation [16]

$$B_m = \frac{B_r}{1+\frac{\mu_r \delta k_c h_m}{l_m l_{iron}}} \frac{h_m}{l_{iron}}, \tag{1}$$

where B_r is the remanent flux density of the permanent magnet, μ_r is the relative magnet permeability, and k_c is the Carter factor given by [19]

$$k_c = \frac{\tau_s}{\tau_s - \sigma_\delta b_{ss1}} \tag{2}$$

$$\sigma_\delta = \frac{2}{\pi}\left\{\arctan\left(\frac{b_{ss1}}{2(\delta+h_m)}\right) - \frac{\delta-h_m}{b_{ss1}} \ln\left[1+\left(\frac{b_{ss1}}{2(\delta+h_m)}\right)^2\right]\right\} \tag{3}$$

where τ_s is the slot pitch and b_{ss1} is the inner stator slot width. The width of a rotor iron piece l_{iron} is calculated by

$$l_{iron} = \left(\frac{\pi}{2} - \alpha\right)\frac{D_{rint}}{2p} \tag{4}$$

where D_{rint} is the rotor inner diameter, p is the number of pole pairs and l_m is the magnet thickness. It is given by

$$l_m = \frac{\alpha D_{rint}}{2p} \tag{5}$$

The amplitude of the fundamental airgap flux density ($B_{\delta 1}$) is calculated by the following equation [2]

$$B_{\delta 1} = \frac{4}{\pi} B_m \sin(\alpha). \tag{6}$$

The flux density in the stator yoke (B_{sy}) is determined by [17]

$$B_{sy} = \frac{B_m \tau_m}{2h_{sy}} \tag{7}$$

where h_{sy} is the stator yoke height and τ_m is the pole width. The flux density in the rotor yoke (B_{ry}) is expressed by [17]

$$B_{ry} = \frac{B_m \tau_m}{2h_{ry}} \tag{8}$$

where h_{ry} is the rotor yoke height. The equations of the flux densities in the wide and narrow teeth, (B_{st1}) and (B_{st2}) are respectively given by [15]

$$B_{st1} = \frac{B_m \tau_s (l+2\delta)}{b_{ts1} l} \tag{9}$$

$$B_{st2} = \frac{B_m \tau_s (l+2\delta)}{b_{ts2} l} \tag{10}$$

The copper loss (P_{co}) is calculated from the windings resistance of a phase, (R_{ph}), and the phase current (I_{ph}) [17]

$$P_{co} = 3R_{ph} I_{ph}^2 \tag{11}$$

The iron losses can be calculated using the following equation [20]

$$P_{iron} = k_{hyst} B^\beta f + k_{eddy} (Bf)^2 + 8.67 k_{exc} (Bf)^{1.5} \tag{12}$$

where k_{hyst} is the hysteresis coefficient, B is the flux density, β is the Steintmetz constant, k_{eddy} is the eddy current coefficient, k_{exc} is the excess eddy current loss coefficient.

To calculate the iron losses in the rotor yoke (P_{ry}), stator yoke (P_{sy}), wide stator teeth (P_{st1}) and narrow stator teeth (P_{st2}), it suffices to replace the value of (B) by the corresponding flux density while multiplying the whole equation by the volume of the corresponding part.

3. Used multiobjective optimization algorithms

3.1 Archive-based hybrid scatter search algorithm: AbYSS

The AbYSS algorithm [21] is based on the scatter search for solving multiobjective problems. The algorithm uses the concepts of external archiving, Pareto dominance and two different density estimators. Moreover, AbYSS incorporates five particular methods, which are: the diversification generation to create an initial set of diverse solutions, the improvement which uses a local search algorithm to improve the new generated solutions, the reference set update to generate new solutions balanced between the diversity and high quality, the subset generation to create new solutions with the combination method between the non-dominated solutions and the other individuals belonging to the diversified solutions, and the solution combination to balance the generation of solutions between the intensification and diversification.

In [21], the AbYSS algorithm has been compared with two multiobjective optimizers, SPEA2 [22] and NSGA-II [23], using 33 unconstrained and constrained test problems. The comparative analysis showed that AbYSS outperforms the other two algorithms according to the diversity of the solutions, and it obtains very competitive results as regards to the hypervolume metric and the convergence towards the true Pareto fronts.

3.2 Cellular genetic algorithm for multiobjective optimization: MOCell

The MOCell algorithm [24] is an evolutionary algorithm for solving multiobjective optimization problems. In this algorithm, each individual of the population belongs to a cell (neighborhood). The parents of the individual, whom it can only recombine with them, are selected only from its neighbors in the cell. This limitation makes it possible to properly control the exploration and exploitation of the search space. If the resulting offspring of the reproduction operation dominate the current individual, then it takes its place at the current position to participate in the reproduction operations of the next generation. Furthermore, the non-dominated solutions are stored in an external archive. If the maximum archive size is reached, the solutions of the archive are then ranked according to the crowding distance and the solutions with the worst values are deleted from the archive. This mechanism obviously makes it possible to preserve the diversity of solutions in the Pareto front.

In [24], the MOCell algorithm has been compared with two state-of-the-art multiobjective optimizers, SPEA2 [22] and NSGA-II [23]; using 21 unconstrained and constrained test problems, and according three quality indicators. The comparative analysis showed that MOCell is very competitive with the other two algorithms considering the hypervolume and convergence measures, and it plainly outperforms as regards to the diversity measure.

3.3 New multiobjective particle swarm optimization: NMOPSO

The NMOPSO algorithm [25] is based on a swarm of particles which move in the search space in order to find the optimal solutions of the multiobjective problem. In the standard PSO algorithms, the displacement of a particle is done by finding a compromise between the best solution visited by the particle (personal leader) and the best solution of its neighborhood (global leader). In the NMPSO approach, the update of the particle velocities is done using a third leader named contemporary leader. Indeed, after the initialization of this leader, the update is done by choosing a random particle from the swarm. If this particle dominates the last contemporary guide, the update will be carried out. This strategy improves the algorithm convergence. Moreover, the speed calculation is done using an adaptive technique. In fact, in the first iterations of the research, this technique encourages the particle to search around itself when the search space is large, which improves the diversity of the particles. In later stages of research, the adaptive technique increase the particle movement of the particles when the search space is small, which improves the convergence accuracy of the algorithm. In this regard, this algorithm focuses on the intelligence of the particle itself at an early stage, and then pays more attention to the intelligence of the entire swarm at a later stage. Moreover, this algorithm uses an external archive to store the optimal solutions found during the search process, and the Pareto dominance and crowding distance to select the best solutions and update the external archive. The NMPSO flowchart is given in Fig. 3.

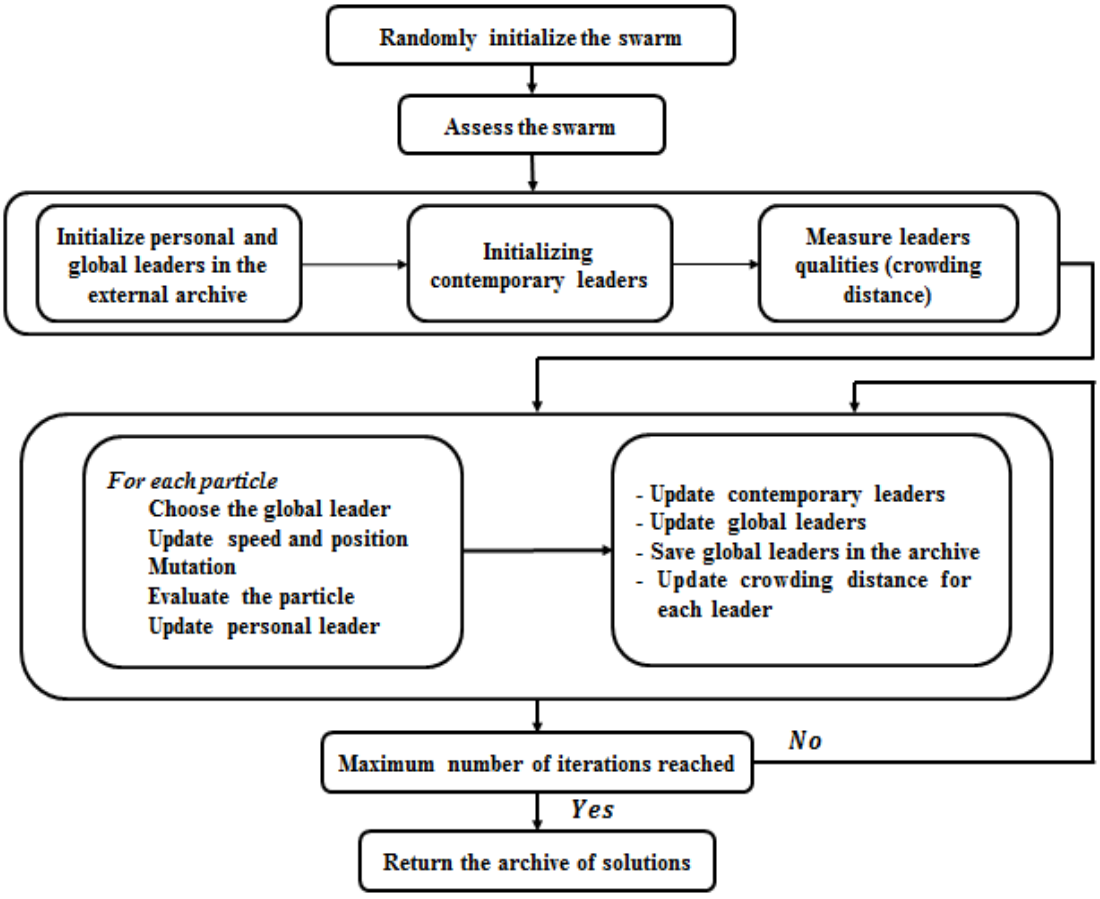

Fig. 3. NMPSO flowchart

In order to find the best algorithm to optimize the geometry of an electric motor, the NMOPSO algorithm has been compared in [17] and [25] with three multiobjective evolutionary algorithms, NSGA-II [23], MOCell [24], and NSGA-III [26], and two multiobjective particle swarm optimization algorithms, OMOPSO [27] and SMPSO [28]. This comparison has been made according to the covariance metric, the hypervolume and the richness of the Pareto front. The results showed that the NMOPSO is the best algorithm according to all performance measures.

4. Optimization of the studied machine

In this section we formulate the multiobjective optimization problem by presenting the decision variables, the objective functions, and the constraints imposed on the machine. Then, we apply the optimization algorithms previously presented in order to find the optimal geometry of the machine.

4.1 Decision variables

The geometry of the machine is well defined by 9 dimensioning parameters. They are: the airgap length, the permanent magnet length, the half pole angle, the widest stator tooth width, the narrowest stator teeth width, the stator slot height, the axial machine length, the stator inner diameter. These geometric parameters are previously exposed in Table 1 and they represent the decision variables of our optimization problem.

4.2 Objective functions

The optimal design of the studied machine is carried out according to three objective functions. The first is to maximize the motor efficiency, the second is to minimize the motor mass and the third is to minimize the torque ripple. These objective functions are given respectively by the following equations

$$obj_{fun1} = minimize(1-\eta) \tag{13}$$

where (η) is the motor efficiency. In order to simplify the problem formulation and improve the quality of Pareto fronts, we treat all objectives as minimization objectives. Indeed, we can transform the efficiency maximization into a minimization objective by subtracting it from 1. By minimizing (1 - η), we are indirectly maximizing η, as the closer η gets to 1, the closer (1 - η) gets to 0. The motor efficiency (η) is calculated based on the output power (P_{out}) and the machine losses by the following equation

$$\eta = \frac{P_{out}}{P_{out}+P_{co}+P_{ry}+P_{sy}+P_{st1}+P_{st2}} \tag{14}$$

$$obj_{fun2} = minimize(mass) \tag{15}$$

$$obj_{fun3} = minimize\left(T_{rip}\right) \tag{16}$$

where (T_{rip}) is the torque ripple of the motor. Indeed, the stator slotting effect influences the magnetic flux distribution in the airgap, resulting in torque ripple. The output torque quality can be improved by reducing the torque ripple [29]. It is calculated by

$$T_{rip} = 2\frac{\sqrt{(\hat{E}_7-\hat{E}_5)^2-(\hat{E}_{13}-\hat{E}_{11})^2-(\hat{E}_{19}-\hat{E}_{17})^2-(\hat{E}_{25}-\hat{E}_{23})^2}}{\hat{E}_1} \tag{17}$$

where $\hat{E}_i$ is the ith harmonic of the back electromotive force and given by [17]

$$\hat{E}_i = 4.44\, f N_c k_{w1} B_{\delta i} \frac{(D_{sext}+\delta)}{p} l \tag{18}$$

where f is the frequency, N_c is number of turns per phase, k_{w1} is the winding factor, $B_{\delta i}$ is the amplitude of the ith harmonic of the air gap flux density and D_{sext} is the stator outer diameter.

4.3 Design constraints

In our multiobjective optimization problem, we applied a set of magnetic constraints in order to avoid the saturation of the magnetic circuit and to define the space of feasible values of the decision variables. These constraints are shown in Table 2. Other design constraints such as: temperature, demagnetization and bulk must be considered in the optimization problem because they directly affect the machine performances and effectiveness. However, these constraints are implicitly considered when imposing magnetic constrains on the allowed induction values. The temperature, demagnetization and bulk constraints will be considered in our future works. In addition, other geometric constraints were considered in the present work. These constraints are illustrated in Table 3 and they are applied to ensure the structure rigidity.

Table 2. Magnetic constraints

Variables	Constrains
Amplitude of the fundamental airgap flux density (T)	$B_{\delta 1} \leq 1.6$
Rotor yoke flux density (T)	$B_{ry} \leq 2$
Stator yoke flux density (T)	$B_{sy} \leq 1.8$
Widest stator tooth flux density (T)	$B_{st1} \leq 2.2$
Narrowest stator tooth flux density (T)	$B_{st2} \leq 2.2$

Table 3. Geometric constraints

Variables	Constrains
Outer stator slot width (mm)	$0.15\ h_s \leq b_{ss2} \leq 0.5\ h_s$
Widest stator tooth width (mm)	$b_{ts1} \geq 1.25\ b_{ts2}$
Narrowest stator tooth width mm)	$b_{ts2} \geq 0.3\ \tau_s$
Stator yoke height (mm)	$h_{sy} \geq 0.5\ h_s$

4.4 Optimization results

In order to implement the multiobjective algorithms previously presented, we used the "jMetal" framework which is developed by the object-oriented java language. As optimization results, we retained respectively the Pareto fronts of the AbYSS, MOCell and NMOPSO algorithms in Fig. 4, Fig. 5 and Fig. 6.

By visualizing the Pareto fronts for these three objectives, the figures provide insights into the trade-offs between efficiency, mass, and torque ripple. Each point on the graph represents a particular solution that optimizes these objectives. The goal is to find solutions that lie on the Pareto front, which represents the best compromise between the objectives. These solutions cannot be improved in one objective without sacrificing performance in another objective. All algorithms have been run multiple times. Indeed, the AbYSS and MOCell algorithms generate 100 solutions at each execution. Otherwise, the NMOPSO algorithm can generate more than 2000 well-diversified solutions in the search space. Moreover, all the points generated by the algorithms are feasible since they respect the imposed constraints and the requirements of the machine. The designer can accordingly choose the solution that meets his needs.

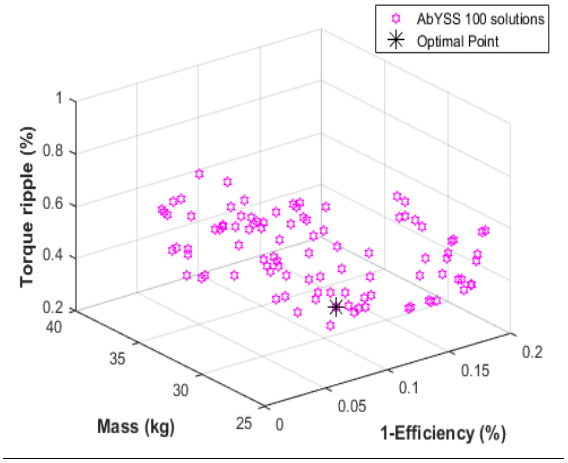

Fig. 4. AbYSS front Pareto

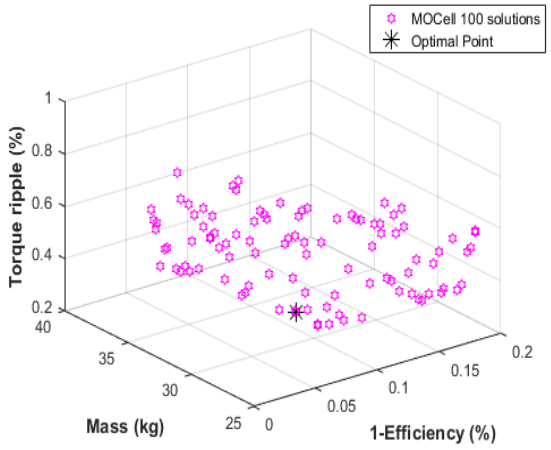

Fig. 5. MOCell front Pareto

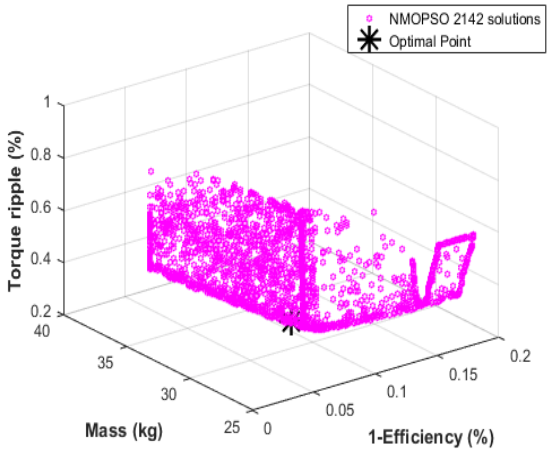

Fig. 6. NMOPSO front Pareto

The most significant results of the machine geometry, relating to the different algorithms, are presented in Table 4. Referring to these results, we can notice that the NMOPSO algorithm can reach the best values of efficiency and torque ripple with a very acceptable mass. Moreover, it presents the lowest execution time knowing that it produces the richest Pareto front.

Table 4. Optimization algorithms results

Parameters	AbYSS	MOCell	NMOPSO
Airgap length (mm)	1.49	1.05	1
Permanent magnet length (mm)	30.44	20.74	20
Half pole angle (Electrical degree °)	2.55	3.73	3.73
Widest stator tooth width (mm)	26	26.70	28.78
Narrowest stator tooth width (mm)	19.14	20.71	19
Stator slot height (mm)	30	31.21	30.15
Axial machine length (mm)	63.09	64.78	63.14
Stator inner diameter (mm)	115.09	121.54	117.57
Efficiency (%)	90.92	92.82	93,35
Mass (kg)	28.19	28.65	28.38
Torque ripple (%)	37.28	37.14	36.41
Execution time (s)	6.736	14.107	6.495

5. Performance evaluation of the machine

To evaluate the performance of the machine, several finite elements analyzes (FEA) are carried out to investigate the optimization results and the distribution of the magnetic field of the studied motor. FEA is known as a powerful tool for analyzing and studying magnetic circuits for electrical machines. This technique is applied in [30] for the parameters estimation of a synchronous generator. To carry out these investigations, we have employed "Ansys engineering simulation software" and we have used the optimization results to define all dimensions and the electromagnetic properties of the machine. Owing to the symmetry and periodicity in the machine structure, the FEA can be limited to a defined study domain. However, in the present study, we are interested to investigate and show the magnetic flux distribution on the machine overall especially in stator teeth and core back. Moreover, the study is limited to 2D which doesn't increase the computation time. The FEA results are presented in Fig. 7 and Table 5.

Table 5. Comparison between FEA and Optimization Results

Parameter	Optimization results	FEA results	Error
The amplitude of the fundamental airgap flux density $B_{\delta 1}$ (T)	1.31	1.37	4.5 %
The rotor yoke flux density B_{ry} (T)	1.83	1.95	6.5 %
The stator yoke flux density B_{sy} (T)	1.19	1.3	9.2 %
The widest stator tooth flux density B_{st1} (T)	1.45	1.4	3.4 %
The narrowest stator tooth flux density B_{st2} (T)	1.72	1.65	4 %

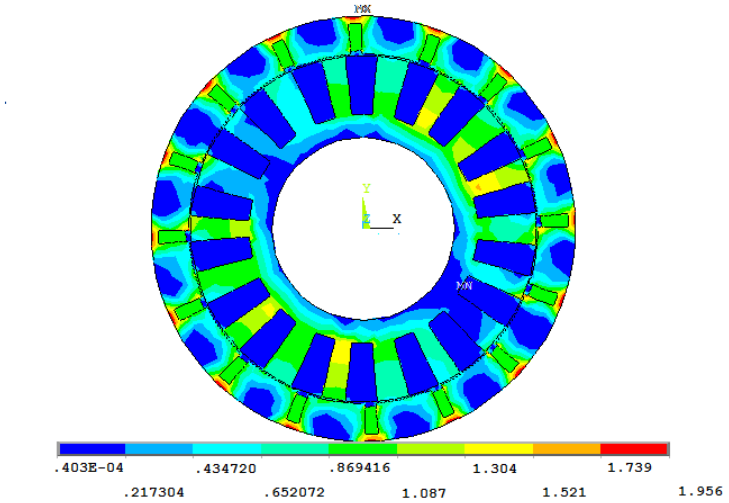

Fig. 7. Total machine induction

By referring to Fig.7, we can observe a magnetic saturation in the rotor yoke and the extremes of permanent magnets. Indeed, it can reach 1.9 Tesla. To limit the magnetic saturation level in the end regions, we can improve the machine design by studying the effect of the rotor core back length on the machine induction. We can, modify the rotor configuration (orientation, location, and shape of the magnets) or applying flux barriers placed on the stator, the rotor, or both. An effective cooling system and heat dissipation mechanisms can also keep the magnetic properties of the materials within acceptable limits. Moreover, we can notice from the Table 5 that there is a good agreement between the optimization results and the FEA results.

6. Conclusion

The work presented in this paper concerns the design and optimization of a permanent magnet synchronous in-wheel motor for an electric vehicle. First, we presented the machine topology. It is a 3-phase, 18 slots, and 16 tangentially magnetized permanent magnets with an outer rotor and unequal stator teeth lapped with single-layer concentrated windings. Then, we developed the analytical calculations of the magnetic flux densities and the iron losses in all parts of the machine. After that, we presented the used optimization algorithms which are the AbYSS, MOCell and NMOPSO algorithms. Moreover, we developed the multiobjective optimization procedure in order to find the optimal design of the studied machine. The optimization results showed that all the algorithms are able to generate a set of feasible solutions and that NMOPSO outperforms the other two algorithms. Finally, the FEM is performed to validate the proposed optimization procedure. All the FEM results prove the rationality of the optimal motor design. The perspectives of this work are multiple, and we propose to refine the analytical design by integrating the thermal, the demagnetization current and the mechanical models in the optimization problem. In addition, the influence of certain parameters on the machine performance will be analyzed. These parameters are: the magnets segmentation and stator slot opening. The machine performances can be also improved by minimizing the iron losses and cogging torque which will be studied in our future works.

References

[1] K. Ramu, Permanent Magnet Synchronous and Brushless DC Motor Drives. Boca Raton, Florida, USA: CRC Press, 2017.

[2] A. Mansouri, “Conception et optimisation multi-objectifs d’un moteur a aimants permanents destine pour un vehicule electrique,” Ph.D. dissertation, University of Gafsa, Tunisia, 2016.

[3] C. Qiping, L. Chuanjie, O. Aiguo, L. Xiangqin, and X. Qiang, “Research and development of in-wheel motor driving technology for electric vehicles,” International Journal of Electric and Hybrid Vehicles, vol. 8, no. 3, pp. 242–254, 2016. [Online]. Available: https://doi.org/10.1504/IJEHV.2016.080024

[4] B. Esra Kandemir, “Electrical equivalent circuit for modelling permanent magnet synchronous motors,” Journal of Electrical Engineering, vol. 72, no. 3, pp. 176–183, 2021. [Online]. Available: https://doi.org/10.2478/jee-2021-0024

[5] M. Mohd Rezal and I. Dahaman, “Optimization of surface-mounted permanent magnet brushless ac motor using analytical model and differential evolution algorithm,” Journal of Electrical Engineering, vol. 70, no. 3, pp. 208–217, 2019. [Online]. Available: https://doi.org/10.2478/jee-2019-0029

[6] S. Xiaodong, S. Zhou, C. Yingfeng, L. Gang, G. Youguang, and Z. Jianguo, "Driving-cycle-oriented design optimization of a permanent magnet hub motor drive system for a four-wheel-drive electric vehicle," IEEE Transactions on Transportation Electrification, vol. 6, no. 3, pp. 1115–1125, 2020. [Online]. Available: https://doi.org/10.1109/TTE.2020.3009396

[7] Z. Zhiwei, "A Compact High Torque Density Dual Rotor Permanent Magnet In-Wheel Motor With Toroidal Windings," in Proceedings of the 22nd International Conference on Electrical Machines and Systems, ser. ICEMS. Harbin, China: IEEE, 2019, pp. 1–5.

[8] G. Si, G. Hong, and X. Jinquan, "Design and Comparison of Six-Phase Fault-Tolerant Interior Permanent Magnet Motor and Surface-Mounted Permanent Magnet Motor for Electric Vehicles," in Proceedings of the 21st International Conference on Electrical Machines and Systems, ser. ICEMS. Jeju, South Korea: IEEE, 2018, pp. 120–125.

[9] F. Yaojing, L. Fang, H. Shoudao, and Y. Ning, "Variable flux outer-rotor permanent magnet synchronous motor for in-wheel direct-drive applications," Chinese Journal of Electrical Engineering, vol. 4, no. 1, pp. 28–35, 2018. [Online]. Available: https://doi.org/10.23919/CJEE.2018.8327368

[10] G. Peng, G. Yuxi, and W. Xiaoyuan, "The design of a permanent magnet in-wheel motor with dual-stator and dual-field-excitation used in electric vehicles," Energies, vol. 11, no. 2, pp. 2–13, 2018. [Online]. Available: https://doi.org/10.3390/en11020424

[11] R. Akinci and M. Polat, "Design and Optimization with Genetic Algorithm of Double Rotor Axial Flux Permanent Magnet Synchronous Motor (TORUS Type) for Electrical Vehicles," In proceeding of the 2019 4th International Conference on Power Electronics and their Applications (ICPEA). IEEE. Elazig, Turkey, 2019.

[12] P. P. C. Bhagubai, J. G. Sarrico, J. F. P. Fernandes and P. J. Costa Branco, "Design, multi-objective optimization, and prototyping of a 20 kW 8000 rpm permanent magnet synchronous motor for a competition electric vehicle," Energies, vol. 13, no. 10, P. 2465, 2020. [Online]. Available: https://doi.org/10.3390/en13102465

[13] Q. Wang, P. Zhao, X. Du, F. Lin and X. Li, "Electromagnetic Vibration Analysis and Slot–Pole Structural Optimization for a Novel Integrated Permanent Magnet In-Wheel Motor," Energies, vol. 13, no. 13, p. 3488, 2020. [Online]. Available: https://doi.org/10.3390/en13133488

[14] Ö. Dal, M.Yıldırım, and H. Kürüm, "Optimization of permanent magnet synchronous motor design by using PSO," In 2019 4th International Conference on Power Electronics and their Applications (ICPEA). IEEE. Elazig, Turkey, 2019.

[15] L. Zaaraoui, A. Mansouri, and N. Smairi, "Design and optimization of an in-wheel unequal stator teeth motor," International Journal of Renewable Energy Research, vol. 12, no. 1, pp. 284–293, 2022. [Online].
Available: https://doi.org/10.20508/ijrer.v12i1.12723.g8397

[16] L. Florence, "Design, optimization and comparison of permanent magnet motors for a low-speed direct-driven mixer," Ph.D. dissertation, Royal Institute of Technology, Stockholm Sweden, 2004.

[17] L. Zaaraoui, "Elaboration d'une nouvelle métaheuristique en vue de la conception optimale d'un moteur électrique," Ph.D. dissertation, University of Gabes, Gabes, 2022.

[18] V. Sarac, "Performance optimization of permanent magnet synchronous motor by cogging torque reduction," Journal of Electrical Engineering, vol. 70, no. 3, pp. 218–226, 2019. [Online]. Available: https://doi.org/10.2478/jee-2019-0030

[19] F. Yan-li and Z. Cheng-ning, "Analytical calculation for predicting the air gap flux density in surface mounted permanent magnet synchronous machine," Journal of Electrical Engineering and Technology, vol. 65, no. 6, pp. 769–777, 2017. [Online]. Available: https://doi.org/10.5370/JEET.2017.12.2.769

[20] M. T. Kakhki, "Modeling of losses in a permanent magnet machine fed by a pwm supply," Ph.D. dissertation, Laval University, Quebec, Canada, 2016.

[21] N. Antonio J., L. Francisco, A. Enrique, D. Bernabe, D. Juan J., and B. Andreas, "Abyss: Adapting scatter search to multiobjective optimization," IEEE Transactions on Evolutionary Computation, vol. 12, no. 4, pp. 439–457, 2008. [Online]. Available: https://doi.org/10.1109/TEVC.2007.913109

[22] E. Zitzler, M. Laumanns, and L. Thiele, "SPEA2: Improving the Strength Pareto Evolutionary Algorithm," in Proceedings of the EUROGEN Conference, Greece, 2001, pp. 95–100.

[23] D. Kalyanmoy, P. Amrit, A. Sameer, and T. Meyarivan, "A fast and elitist multiobjective genetic algorithm: Nsga-II," IEEE Transactions on Evolutionary Computation, vol. 6, no. 2, pp. 182–197, 2002. [Online].
Available: https://doi.org/10.1109/4235.996017

[24] N. Antonio J., D. Juan J., L. Francisco, D. Bernabe, and A. Enrique, "Mocell: A cellular genetic algorithm for multiobjective optimization," International Journal of Intelligent Systems, vol. 24, no. 7, pp. 726–746, 2009. [Online].
Available: https://doi.org/10.1002/int.20358

[25] L. Zaaraoui, A. Mansouri, and N. Smairi, "Nmopso: an improved multiobjective pso algorithm for permanent magnet design," Scientific Bulletin Series C: Electrical Engineering and Computer Science, vol. 84, no. 1, pp. 201–214, 2022. [Online]. Available: https://www.scientificbulletin.upb.ro/rev_docs_arhiva/fullfec_321988.pdf

[26] D. Kalyanmoy and J. Himanshu, "An evolutionary many-objective optimization algorithm using reference point based non-dominated sorting approach, part i: Solving problems with box constraints," IEEE Transactions on Evolutionary Computation, vol. 18, no. 4, pp. 577–601, 2014. [Online]. Available: https://doi.org/10.1109/TEVC.2013.2281535

[27] R. S. Margarita and C. C. Carlos A., "Improving PSO based Multi-Objective Optimization using Crowding, Mutation and e –Dominance," in Proceedings of the 3rd International Conference on Evolutionary Multi-Criterion Optimization, ser. EMO 2005. Mexico: Springer, 2005, pp. 505–519.

[28] A. Nebro, J. J. Durillo, J. G. Nieto, C. A. Coelle, F. Luna, and E. Alba, "SMPSO: A New PSO-based Metaheuristic for Multi-objective Optimization," in Proceedings of the 2009 IEEE Symposium on Computational Intelligence in Multi-Criteria Decision-Making, ser. MCDM. USA: Nashville, TN, USA, 2009, pp. 66–73.

[29] R. Islam, I. Husain, A. Fardoun, and K. McLaughlin, "Permanent-Magnet Synchronous Motor Magnet Designs With Skewing for Torque Ripple and Cogging Torque Reduction," IEEE Transactions on Industry Applications, vol. 45, no. 1, pp. 152-160, 2009. [Online]. Available: https://doi.org/10.1109/TIA.2008.2009653

[30] H. Msaddek, A. Mansouri, and H. Trabelsi, "Optimal design and cogging torque minimization of a permanent magnet motor for an electric vehicle," Technical Gazette, vol. 30, no. 2, pp. 538–544, 2023. [Online]. Available: https://doi.org/10.17559/TV-20220815140808

Lassaad Zaaraoui was born in Gafsa, Tunisia, in 1991. He received the MSc degree in Embedded Systems and Computer Networks from the Faculty of Sciences of Gafsa, Tunisia, in 2016, and the PhD degree in Electrical Engineering from the National Engineering School of Gabes, Tunisia in 2022. His research interests include electrical machines and optimization algorithms.

Ali Mansouri was born in Kasserine, Tunisia, in 1978. He received the MSc degree in Automatic Industrial Computing from National Engineering School of Sfax, Tunisia in 2003, the PhD degree in Electrical Engineering from the same university in 2010 and the HDR degree in Electrical machine design and optimization in 2016 from the University of Gafsa. He is currently a lecturer in the Department of Electrical Engineering, Higher School of Applied Sciences and Technology of Gafsa, Tunisia. His research interests are related to the analysis and design of electrical machines.